On a new method of evaluation of the inelastic state due to moving contact

Nada Maouche, Habibou Maitournam, Ky Dang Van

On a new method of evaluation of the inelastic state due to moving contacts

N. Maouche, M.H. Maitournam, K. Dang Van

Laboratoire de Mécanique des Solides, CNRS URA 317, Ecole Polytechnique, 91128 Palaiseau Cedex, France

The prediction of damage and wear of materials under repeated moving contacts requires first the determination of the limit response in terms of stress and strain. The simulation necessary to calculate the limit response could be performed with classical finite elements and an incremental treatment of the loading history, resulting in lengthy and repeated calculations. For steady-state moving contacts, the stationary methods allow a quick evaluation of the stabilized state. These procedures cannot be used in the case of an arbitrary cyclic loading resulting, for example, from small oscillatory contacts. In this paper, a new finite element approach is developed for structures subjected to an arbitrary cyclic loading. It is based on an original integration scheme which allows direct determination of the stabilized state of stresses, strains and internal parameters. This asymptotic state could be either an elastic shakedown, a plastic shakedown or ratchetting for an elastic-plastic material. Elastic and plastic shakedown states are easily obtained with this method. Applications to fretting fatigue and wear in relation to material fatigue properties are presented.

Keywords: Numerical method; Fretting; Fatigue; Crack nucleation

1. Introduction

Fretting is the surface damage induced by small amplitude oscillatory displacements between metal components in contact. Depending on the imposed forces or the displacement amplitude, damage can either be wear or crack nucleation. Many experimental results have been obtained in recent years. Vingsbo et al. [1] and Vincent et al. [2] have established a test methodology based on fretting maps. These maps give the material response fretting map (MRFM) (no damage, crack nucleation or wear) according to the running condition fretting map (RCFM) (partial slip and gross regime). They are very useful for qualitative understanding of damage phenomena. However, the results obtained cannot be applied to another set-up having different solid geometries and material properties. Thus, the use of an intrinsic methodology to predict fretting is essential. For this purpose, our approach is based on numerical calculations and a multiaxial fatigue criterion. It takes account of the geometries of solids in contact and material properties and can be applied to any kind of structure under fretting. The prediction of damage by numerical simulation requires one first to compute the mechanical quantities resulting from the cyclic contact loading due to fretting. The type of loading [3–5] is either a moving contact loading or a contact fixed in space but varying in time. The incremental method based on a step by step integration could be used to calculate the possible stabilized state resulting in lengthy calculations. A new method is proposed to avoid this inconvenience. The stabilized state is obtained directly by an original integration scheme taking advantage of the periodicity of the loading path. This method is applied for the two cases of loading discussed above to simulate a fretting-fatigue set-up. The stabilized mechanical state is determined. It is shown that plastic shakedown is associated with wear (gross slip regime) while elastic shakedown leads to crack nucleation. The Dang Van criterion is used to predict this nucleation.

* Tel.: +33 1 69 33 33 40; e-mail maouche@athena.polytechnique.fr

2. Description of the loading

Let us consider two bodies in contact under a normal constant compressive force P and subjected to a repeated alternating tangential force $T(t)$. In order to calculate the elastoplastic limit response of the material in fretting, we describe first the loading cycle. Although the aim of the numerical method is to evaluate the inelastic state, the normal pressure and the shear tractions are assumed to be given respectively by the elastic theory of Hertz and the theory of Mindlin. This approximation is valid when the stabilized state is elastic (elastic shakedown). In the case of plastic shake-

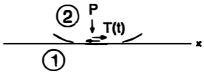

Fig. 1. Model of calculations.

down, the contact pressures are in fact modified during the cycles but the hypothesis of elastic contact pressures is maintained.

The contact width is assumed to be sufficiently small in comparison with the dimensions of the two bodies. Body 1 is represented as a half space (Fig. 1). The constant normal pressure $p(x)$ and the contact area are assumed to be given by Hertz theory:

$$p(x) = p_0\sqrt{1-\frac{x^2}{a^2}}$$

where p_0 is the maximum normal pressure and a is the contact half-width. The tangential force $T(t)$ describes an alternate loading cycle of amplitude $2T_{max}$. Two cases are studied.

$T_{max} < \mu P$. No full slip occurs during the loading cycle if T_{max} is less than μP, where μ is the friction coefficient. The distribution of the shear traction is given by Mindlin theory [6]. The contact zone is divided into a central sticking zone of width c bordered by slipping zones which vary with the tangential force $T(t)$. The loading cycle is represented by the shear traction distributions shown in Fig. 2. In the configurations A and B, the tangential force $T(t)$ decreases from T_{max} to 0 in C, still decreases in the configuration D and reaches $-T_{max}$ in E. At the instant E, $T(t)$ increases from $-T_{max}$ to 0 in the configuration G and reaches T_{max} in H. The shear traction distributions are provided by the following equations:

$$\begin{cases} q(x) = -\mu p_0\sqrt{1-\dfrac{x^2}{a^2}} & c \le |x| \le a \\ q(x) = -\mu p_0\left[\sqrt{1-\dfrac{x^2}{a^2}} - 2\dfrac{c}{a}\sqrt{1-\dfrac{x^2}{c^2}}\right] & c_{max} \le |x| \le c \\ q(x) = -\mu p_0\left[\sqrt{1-\dfrac{x^2}{a^2}} - 2\dfrac{c}{a}\sqrt{1-\dfrac{x^2}{c^2}} + \dfrac{c_{max}}{a}\sqrt{1-\dfrac{x^2}{c_{max}^2}}\right] & |x| \le c_{max} \end{cases}$$

where c_{max} is given by

$$\frac{c_{max}}{a} = \sqrt{1-\frac{T_{max}}{\mu P}}$$

and c is a function of T:

$$\frac{c}{a} = \sqrt{1-\frac{T_{max}-T}{2\mu P}}$$

$T_{max} = \mu P$. Full slip arises during the loading cycle if T_{max} is equal to μP [7]. The shear traction distributions are shown in Fig. 3. In the configurations A, B and C illustrated in Fig. 3, the contact loading is fixed in space but the tangential force increases from 0 to T_{max}. When T_{max} is reached, the contact loading slides in the direction of positive x with a displacement. In the configurations D, E and F shown also in Fig. 3, the tangential force decreases from $-T_{max}$ to T_{max} and the loading is fixed in space. When $-T_{max}$ is reached, the contact loading moves with a distance δ in the direction of negative x. Finally, in configurations G and H, $T(t)$ increases from $-T_{max}$ to 0. Shear tractions are then given by the following equations:

$$\begin{cases} q(x) = -\mu p_0\sqrt{1-\dfrac{x^2}{a^2}} & c \le |x| \le a \\ q(x) = -\mu p_0\left[\sqrt{1-\dfrac{x^2}{a^2}} - 2\dfrac{c}{a}\sqrt{1-\dfrac{x^2}{c^2}}\right] & |x| < c \end{cases}$$

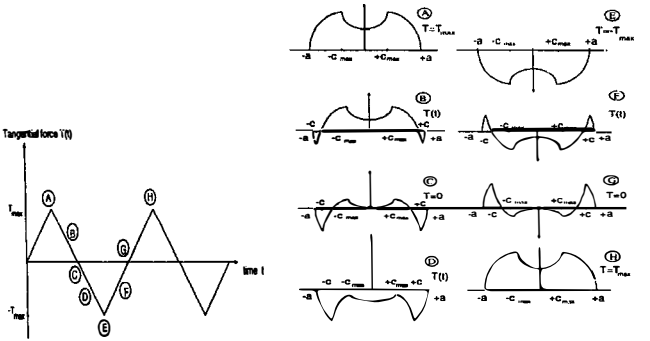

Fig. 2. Loading cycle without full sliding and the corresponding shear traction distributions.

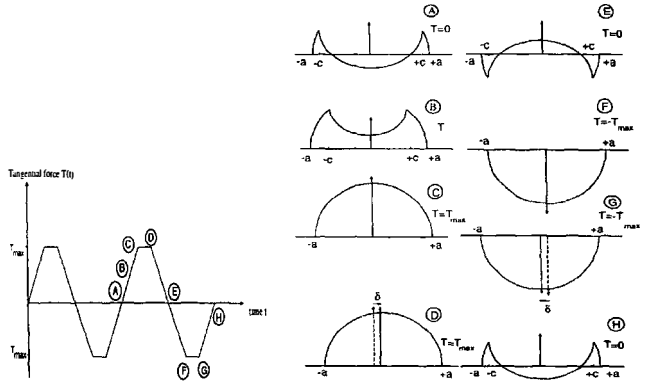

Fig. 3. Loading cycle with full sliding and the corresponding shear traction distributions.

where c is still function of T as:

$$\frac{c}{a}=\sqrt{1-\frac{T_{max}-T}{2\mu P}}$$

The cycles of loading just described are prescribed as external forces for the determination of the stabilized state with the new numerical method which is now presented

3. Numerical method

The stabilized mechanical response of body 1 is either a shakedown or a ratchetting since the loading is periodic. Knowledge of the evolution is only of limited interest. The cyclic direct method allows the determination of the asymptotic response of the structure without following the loading step by step.

The material considered is elastoplastic with kinematic hardening. $\boldsymbol{F}^d(t)$ denotes ($t\in[0,T]$) the external loading path of period T corresponding to either fixed or moving contact as described above. The interval $[0,T]$ is discretized in n intervals $0<t_1<\ldots<t_n=T$.

In the incremental method, for each loading increment $\Delta\boldsymbol{F}^d$, the incremental quantities $\Delta\sigma$, $\Delta\epsilon$, $\Delta\epsilon^p$ are evaluated such as to satisfy static and kinematic admissibility conditions. The loading path is followed until the limit response is reached.

Following ideas of Ladevèze [8,9] and Akel and Nguyen [10], we seek directly the asymptotic response. The approach used is iterative. For each iteration j, at time t_i, we first seek the stress tensor σ_i^{js}, which is statically admissible with the loading $\boldsymbol{F}^d(t_i)$ and the strain tensor ϵ_i^j, which is kinematically admissible with the prescribed displacements $\boldsymbol{U}^d(t_i)$ corresponding to the instant t_i. These two conditions are equivalent to the resolution of equilibrium equations:

$$\boldsymbol{K}\boldsymbol{U}_i^j=\boldsymbol{Q}_i+\boldsymbol{Q}_i^{p^{j-1}}$$

in which $\boldsymbol{Q}_i$, $\boldsymbol{Q}_i^{p^{j-1}}$ and $\boldsymbol{K}$ represent the nodal external forces corresponding to $\boldsymbol{F}^d(t_i)$, the vector of the loads due to plastic strain $\epsilon_i^{p^{j-1}}$ (assumed known) and the stiffness matrix of the linear elastic structure respectively.

In a second stage, we determine the stress tensor σ_{i+1}^{jp} plastically admissible. At each time, the plastic strain ϵ_{i+1}^{jp} is obtained by projecting the strain increment $\epsilon_{i+1}^j-\epsilon_i^j$ on the elastic convex domain defined by the initial state $(\sigma_i^{jp},\epsilon_i^j,\epsilon_i^{p^j})$ attimet_i which is known. σ_{i+1}^{jp} is then calculated from the constitutive law written in incremental form:

$$\epsilon_{i+1}^j-\epsilon_i^j=\boldsymbol{K}(\sigma_{i+1}^{jp}-\sigma_i^{jp})+(\epsilon_{i+1}^{pj}-\epsilon_i^{pj})$$

The stabilized state is obtained when the plastic strain ϵ_1^{pj} at the beginning of the cycle is the same as that at the end of the cycle ϵ_n^{pj}. Otherwise, the same steps are performed in iteration $j+1$ by initializing ϵ_1^{pj+1} to ϵ_n^{pj} and the process is repeated until elastic or plastic shakedown is achieved. Ratchetting is revealed by the non-convergence of the procedure.

4. Comparison between the numerical results obtained with the cyclic direct method and the incremental method

The applicability of the method is illustrated with two-dimensional examples. The numerical results and the times of computation obtained by the cyclic direct method are compared with those obtained by the classical incremental method in the case of a sticking regime loading cycle and full sliding

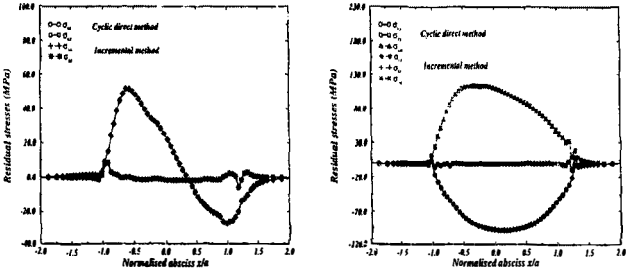

Fig. 4. Comparison of the residual stresses at the surface in the case of full sliding

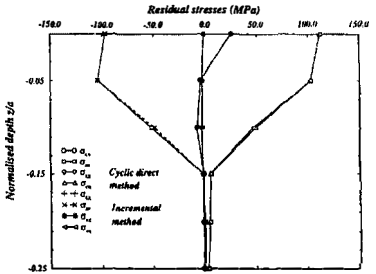

Fig. 5. Comparison of the residual stresses in the depth in the case of full sliding.

loading cycle. Computations are done on an HP 700 work station. A mesh of 4539 nodes is used to represent the half-space. The smallest element size is $0.05a$. The body is made of elastoplastic Von Mises material with linear kinematic hardening. The material parameters are indicated below.

Young's modulus E	207 GPa
Poisson's coefficient ν	0.3
Shear resistance k	159.118 MPa
Hardening modulus C	30 GPa

The computation with the gross slip loading is performed with the parameters given below leading to plastic shakedown.

Ratio of normal pressure p_0/k	2
Coefficient of friction μ	0.6
Amplitude of displacement δ/a	0.2

The stabilized state (plastic shakedown) is obtained with the incremental method after 30 h of CPU time (74 cycles) while it requires only a CPU time of 3 h with the cyclic direct method. The new method runs in this case 10 times faster

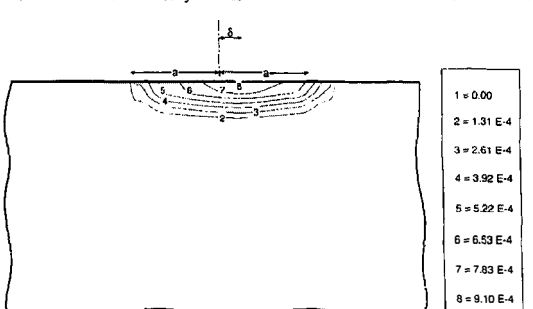

Fig. 6. Contours of equivalents plastic strain in the case of full sliding.

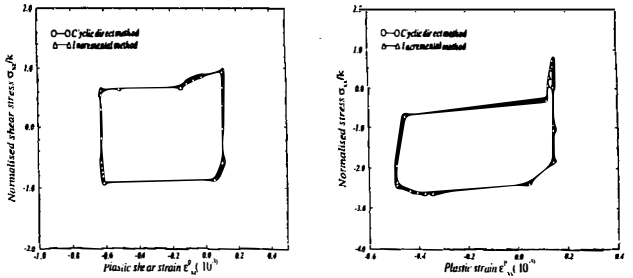

Fig. 7. Comparison of stress–plastic strain cycles in the case of full sliding.

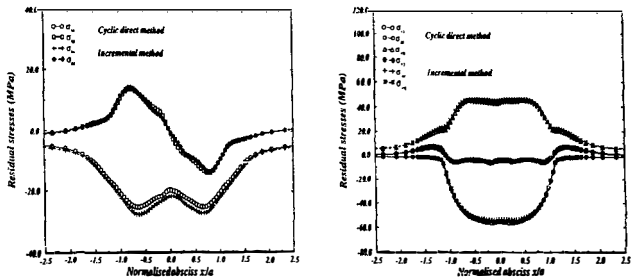

Fig. 8. Comparison of the residual stresses at the surface in the sticking regime.

than the incremental method. The components of the residual stress obtained by the incremental method and the cyclic direct method at the surface and in the depth are compared in Fig. 4 and Fig. 5. A good agreement between the numerical results is found. The contours of equivalent plastic strain are shown in Fig. 6, illustrating a surface flow under the contact zone. In Fig. 7, the stabilized cycles of stress vs. plastic strain of an element at the edge of the contact surface obtained with the two methods are plotted. A good agreement is also found. The loading corresponding to the stick–slip regime is analyzed with the parameters given below.

Ratio of normal pressure p_0/k	3.5
Coefficient of friction μ	0.3
Tangential force T_{max}/P	0.25

The stabilized state (elastic shakedown) is obtained with the incremental method in 50 min CPU time and in 23 min by the cyclic direct method. The components of the residual stresses obtained with the two methods are plotted at the surface in Fig. 8 and as a function of depth in Fig. 9, showing good agreement. The contours of equivalent plastic strain are

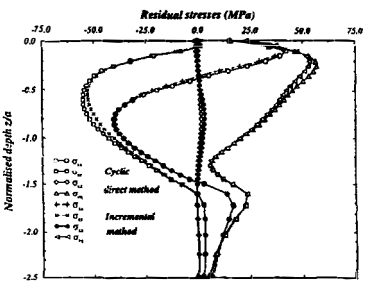

Fig. 9. Comparison of the residual stresses in the depth in the sticking regime.

shown in Fig. 10. The maximum plastic strain is reached in the subsurface at a depth of $0.5a$ under the contact zone. For this depth, the stress vs. plastic shear strain and the stress vs. shear strain cycles computed by the two methods are plotted in Fig. 11 illustrating a satisfying concordance.

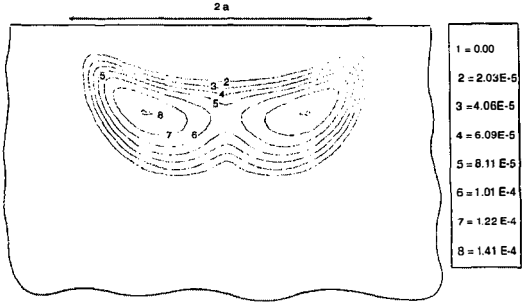

Fig. 10. Contours of equivalent plastic strain in the sticking regime.

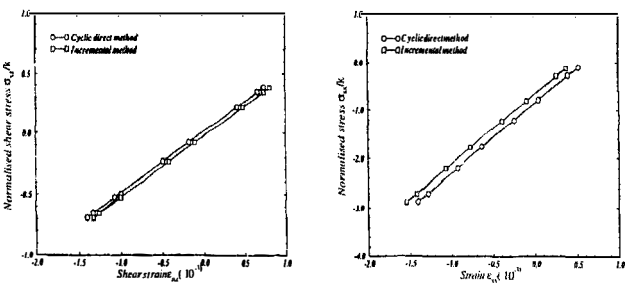

Fig. 11. Comparison of stress–strain cycles in the sticking regime.

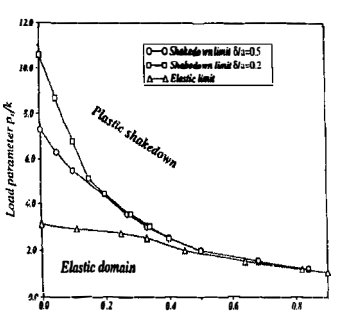

Fig. 12. Shakedown map.

For displacement amplitudes of $\delta = 0.2a$ and $\delta = 0.5a$, the variation of shakedown limit with the ratio of the normal pressure and the friction coefficient is shown in Fig. 12. It is noticed that, for a low friction coefficient, the shakedown limit is reached for high normal pressures ($10k$). Indeed, although the normal pressure is high, the stress amplitude is low because of the small displacement amplitude and the low friction coefficient. As is usually recognized, it is the amplitude of stresses which governs effectively the shakedown.

Notice also, that for high coefficients of friction, the shakedown limits for $\delta = 0.2a$ and $\delta = 0.5a$ are the same and are nearly equal to the elastic limit.

5. Application to fretting fatigue

The experimental set-up is presented in [11]. Two cylindrical fretting pads (diameter 10 mm) are clamped against

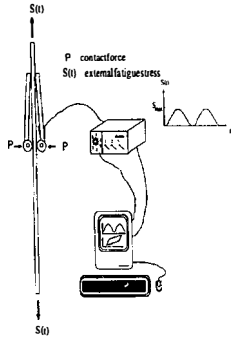

Fig. 13. Fretting-fatigue set-up.

the two surfaces of a flat uniaxial fatigue specimen tested under constant amplitude loading at a frequency of 20 Hz as shown in Fig. 13. The pads are made of 100C6 steel and the fatigue specimen is made of 3Cr–MoV steel. The mechanical properties are given below.

	Yield strength (MPa)	Tensile strength (MPa)	Young's modulus (GPa)	Hardness (HV)
3Cr–MoV	980	1140	215	360
100C6	1700	2000	210	62

The prescribed oscillatory displacement between the pads is linked to the prescribed oscillatory fatigue stress $S(t)$ in the specimen. For a maximum stress $S_{max} = 500$ MPa, the amplitude of displacement is 0.55 μm. The flexible beams are equipped with strain gauges in order to measure the clamping force P between pads and specimen and the friction force related to the accommodation displacements. The variations of the tangential force $T(t)$ are recorded for each fatigue cycle and plotted as a function of fretting fatigue stress $S(t)$ (fretting fatigue loops). By varying the operating parameters (P, S_{max}), three regimes are established.

- The sticking regime. Fretting fatigue loops keep a non-evolutive closed shape. The loops are quite linear during the test. The macroscopic displacement between the contacting surfaces is mainly accommodated by elastic deformation in the near surface of the two components. No damage (wear or crack nucleation) appears during the 10^7 cycles of the test.
- Mixed stick–slip regime. The loops present an elliptical closed shape. There is partial slip and fatigue crack nucleation observed at the edges of the contact.

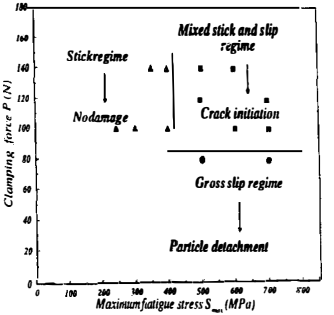

Fig. 14. Fretting fatigue map.

- Gross slip regime. The loops present a trapezoidal shape. Full slip occurs between the two contacting surfaces. In this regime, particle detachment is observed.

The different regimes are obtained for varying parameters (P, S_{max}) summarized in the map shown in Fig. 14.

6. Numerical analysis and prediction of wear and crack nucleation

The prediction of damage mechanisms shown in the map, Fig. 14, requires first the calculation of the stress history in the stabilized state. Secondly, the Dang Van multiaxial fatigue criterion is applied if the stabilized state is elastic shakedown.

Petiot et al. [11] used the incremental method to calculate the stresses. The finite element method described in Section 3 is used here to simulate the set-up and to calculate the stress history in the stabilized state. The specimen is modelled as a half-space subjected to a constant normal force and a varying tangential force $T(t)$ and a fatigue stress $S(t)$ varying linearly with $T(t)$. The material is elastoplastic with kinematic hardening (hardening modulus $C = 30$ GPa) and with properties given in Section 5.

Three simulations are performed corresponding to the three regimes established in the map (P and S_{max} are the prescribed parameters and T_{max} is measured in the test):

- sticking regime, $P = 140$ N, $S_{max} = 350$ MPa and $T_{max} = 53$ N (no damage);
- mixed stick–slip regime, $P = 100$ N, $S_{max} = 600$ MPa and $T_{max} = 80$ N (crack nucleation);
- gross slip regime, $P = 80$ N, $S_{max} = 500$ MPa and $T_{max} = 64$ N (wear).

In the case of loading in the gross slip regime, the non-linear stress–plastic strain cycles for an element located at the surface under the contact zone ($x = -0.4a$) are shown in Fig. 15, illustrating plastic shakedown. Wear is then associ-

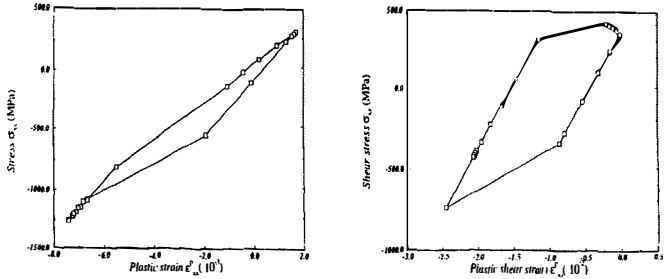

Fig. 15. Stress–plastic strain cycles in fretting fatigue (gross slip).

ated with plastic shakedown and so with low cycle fatigue properties confirming the works of Kim and Ludema [12] and Johnson [13]. Owing to this numerical method, we obtain, better still, the plastic strain amplitude in the stabilized state.

Since the response of the material is respectively purely elastic and elastic shakedown in the sticking regime and mixed stick–slip regime, high cycle fatigue is of concern. The stress cycle through the contact is multiaxial. Uniaxial empirical high cycle fatigue criteria are not applicable. As in [11], the Dang Van multiaxial fatigue crack nucleation criterion is used to predict fatigue cracks. It involves comparing the loading path described by the microscopic shear τ and the pressure p with the fatigue properties of the material obtained by torsion t and bending f fatigue tests ($t = 380$ MPa and $f = 594$ MPa for 30NCD16 steel). More details about the Dang Van multiaxial fatigue crack nucleation criterion are given in Refs. [14,15]. The most critical point is located in the surface at the edge of the contact. The most critical loading path (τ,p) for each regime resulting from the stress cycles in the stabilized state is plotted in Dang Van's fatigue diagram shown in Fig. 16. In the sticking regime, the loading path (τ,p) is beneath the fatigue line material, so no damage occurs. In the mixed stick–slip regime, the loading path intersects the fatigue line material concluding with crack failure. The prediction of crack initiation is in good agreement with the experimental observations.

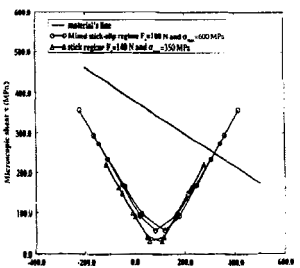

Fig. 16. Loading path in Dang Van's diagram in stick regime and mixed stick–slip regime.

7. Conclusion

A new finite element method is developed to evaluate the inelastic state of structures subjected to cyclic loading. The stabilized state (elastic or plastic shakedown) is obtained directly by an original scheme of integration. Application to fretting is presented with alternate moving contacts. Two kinds of cyclic loading encountered in fretting are considered: an alternate moving contact with small amplitude of displacement corresponding to the gross slip regime, and a fixed contact in space but varying in time corresponding to the sticking regime. This method avoids lengthy repeated calculations required by the classic incremental method. The calculations in the direct cyclic method can be 10 times faster than the incremental method. The results obtained in the stabilized state with the two methods are compared and a good agreement is noted.

Numerical analysis is performed with the direct cyclic numerical method to simulate a fretting fatigue set-up and evaluate the mechanical characteristics. It is found that wear in the gross slip regime is associated with plastic shakedown and therefore to low cycle fatigue properties. Calculations in sticking and mixed stick–slip regimes lead respectively to purely elastic and elastic shakedown. A multiaxial fatigue criterion is used to predict nucleation, and good agreement with experimental observations is found. The numerical direct cyclic method combined with Dang Van multiaxial fatigue crack nucleation allows the prediction of the fretting fatigue map in relation to material properties. Our approach, based on numerical calculations and a multiaxial fatigue criterion, takes account of solid geometries in the contact and

material properties and so it is a promising method for prediction of the damage of structures under fretting.

References

[1] O. Vingsbo and S. Söderberg, On fretting maps, *Wear, 126* (1988) 131–147.

[2] L. Vincent, Y. Berthier and M. Godet, Testing methods in fretting fatigue: a critical appraisal, standardisation of fretting fatigue test methods and equipment. In M. Helmi Attia and R.B. Waterhouse (eds.), *ASTM STP 1159*, American Society for Testing and Materials, Philadelphia, PA, 1992, pp. 33–48.

[3] K. Dang Van and M.H. Maitournam, Steady-state flow in classical elastoplasticity: application to repeated rolling and sliding contact, *J. Mech. Phys. Solids, 41* (11) (1993) 1691–1710.

[4] K. Dang Van and M.H. Maitournam, Thermomechanical state near rolling contact area. In D. Dowson et al. (eds.), *Dissipative Processes in Tribology*, Elsevier, Amsterdam, 1994, pp. 423–428.

[5] K. Dang Van and M.H. Maitournam, Elastoplastic calculations of the mechanical state in alternative moving contacts: application to fretting fatigue. In R.B. Waterhouse and T.C. Lindley (eds.), *Fretting Fatigue*, ESIS 18, Mechanical Engineering Publications, London, 1994, pp. 161–168.

[6] R.D. Mindlin, Compliance of elastic bodies in contact, *J. Appl. Mech., 16* (1949) 259–268.

[7] K.L. Johnson, *Contact Mechanics*, Cambridge University Press, Cambridge, 1985.

[8] P. Ladevèze, La methode à grand increment pour l'analyse de structures à comportement non linéaire décrit par variables internes, *C.R.A.S 309, Sér. II, no. 11*, 1989, pp. 1095–1099.

[9] Ph. Boisse, P. Ladevèze and P. Rougée, A large time increment method for elastoplastic problems, *Eur. J. Mech. A, 4* (1989) 257–275.

[10] S. Akel and Q.S. Nguyen, Determination of the limit response in cyclic plasticity. In D.R.J. Owen, E. Hinton and E. Onate (eds.), *Proc. 2nd Int. Conf. on Computational Plasticity: Models, Software and Applications*, Pineridge Press, Swansea, 1989, pp. 639–650.

[11] C. Petiot, L. Vincent, K. Dang Van, N. Maouche, J. Foulquier and B. Journet, An analysis of fretting-fatigue failure combined with numerical calculations to predict crack nucleation, *Wear, 181–183* (1995) 101–111.

[12] K. Kim and K.C. Ludema, A correlation between low cycle fatigue and scuffing properties of 4340 steel, *Wear, 117* (1995) 617–621.

[13] K.L. Johnson, Contact mechanics and wear of metals, *Wear, 190* (1995) 162–170.

[14] K. Dang Van, B. Griveau and O. Message, On a new multiaxial fatigue limit criterion: theory and application, biaxial and multiaxial fatigue. In M.W. Brown and K. Miller (eds.), *EGF Publication 3*, 1982, pp. 479–496.

[15] K. Dang Van, Macro-micro approach in high-cycle multiaxial fatigue. In D.L. McDowell and R. Ellis (eds.), *Advances in Multiaxial Fatigue, ASTM STP 1991*, American Society for Testing and Materials, Philadelphia, PA, 1993, pp. 120–130.